Pergamon

Int. J. Solids Structures Vol. 32, No. 3/4, pp. 357–373, 1995

0020–7683/95 $9.50 + .00

0020–7683(94)00123–5

A FLEXIBLE RECTANGULAR FOOTING ON A GIBSON SOIL: REQUIRED RIGIDITY FOR FULL CONTACT

J. P. DEMPSEY
Department of Civil and Environmental Engineering, Clarkson University, Potsdam, NY 13699-5710, U.S.A.

and

HUI LI
Sargent and Lundy Engineers, 55 E. Monroe, Chicago, IL 60603, U.S.A.

(*Received* 17 *June* 1994)

Abstract—The problem of a rectangular footing or a strip footing resting on a nonhomogeneous elastic half-space is studied in this paper. The medium is assumed to be isotropic with a shear modulus linearly increasing with depth $G(z) = G_0 + mz$ and a constant Poisson's ratio equal to 1/3. An important feature of this model is that either the Winkler foundation or the elastic homogeneous half-space can be made special cases by letting G_0 or m equal zero, respectively—some results are presented for these cases. In order to investigate the necessary conditions for a footing to be considered rigid, both rigid and flexible footings have been studied. Central concentrated (column) loading, in addition to the self-weight, is treated—being the most demanding in terms of the zero uplift requirement (under conditions of symmetry in the loading with respect to the plate geometry, imposed for reasons of mathematical feasibility). The contact is assumed to be tensionless. There are three important steps in this formulation. The fundamental solution of the nonhomogeneous half-space is separated into the fundamental solution of the homogeneous half-space and a function related to the nonhomogeneity of the half-space. The latter function is approximated by an analytically tractable expression. The contact region is discretized using an adaptive scheme that accounts for the possible edge and corner singularities. The latter scheme removes the burden of most of the numerical integration. A rigid strip footing and a rigid rectangular footing are treated first to ascertain the convergence of the solution procedure and to provide information requisite for the flexibility study. The title problem is transformed into the solution of three coupled two-dimensional singular integral equations. The contact regions are found iteratively since the problem is nonlinear.

INTRODUCTION

Nonhomogeneous soil subgrades are widely encountered in geotechnical engineering, perhaps more commonplace than homogeneous soil. Because of the different consolidation histories, the surface soil tends to have a lower elastic modulus than the deeper soil (Burland *et al.*, 1973). To model this type of phenomenon, a nonhomogeneous elastic half-space with a linearly varying shear modulus $G(z) = G_0 + mz$ and a constant Poisson's ratio has been used by many researchers (Gibson, 1974). The model reduces to a homogeneous half-space when $m = 0$. On the other hand, the model behaves like a Winkler foundation when $G_0 = 0$: a load at one point has no effect on the surface displacement at another point. Based on the above model, many loading cases of interest to geotechnical engineering have been studied, e.g. uniform strip surface load (Gibson, 1969; Gibson *et al.*, 1971; Brown and Gibson, 1972), a uniform rectangular surface load (Brown and Gibson, 1973), uniform circular surface load (Brown, 1969; Gibson *et al.*, 1971), a rigid circular surface footing (Carrier and Christian, 1973; Brown, 1974), and a flexible circular footing (Boswell and Scott, 1976). In addition, a nonhomogeneous elastic layer has also been studied (Brown and Gibson, 1979). The primary information sought is the surface settlement and contact pressure. The moments and shear forces within the footing can be calculated once the contact pressure distribution is known.

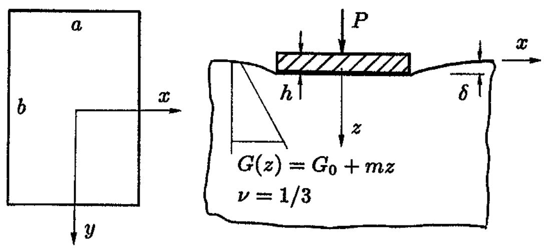

Fig. 1. A rectangular footing on a nonhomogeneous elastic half-space.

The principal aim of this paper is to study the cases of rectangular and strip footings on a nonhomogeneous elastic half-space (Fig. 1). The fundamental solution for the surface displacement due to a point load can be deduced from Awojobi and Gibson (1973). By using this solution, the problem of a rigid rectangular footing on a nonhomogeneous elastic half-space is reduced to the solution of an integral equation with the contact pressure as the unknown function. Furthermore, by extending the formulation given by Li and Dempsey (1988), a flexible footing on the foundation is also treated. By studying flexible footings, it is possible to show the influence of flexibility on the resulting settlement and contact pressure. In so doing, an indication is provided of the footing rigidity needed for the rigid-footing assumption to be valid. A special scheme has been used to treat the contact pressure singularities at the corners and edges.

ANALYTICAL CONSIDERATIONS

The present work applies a similar numerical scheme to that adopted by Dempsey and Li (1989a,b) to determine contact pressure distributions, deflections and contact regions for the case of a flexible rectangular footing resting on a nonhomogeneous half space. The contact is assumed to be smooth and frictionless. The loading is specified to have two axes of symmetry and to be centrally located on the footing. The contact stresses are constrained to be either compressive or zero. In other words, uplift or separation of the footing is not prevented. Significant factors include the ratio of the footing's flexural rigidity to the compliance of the nonhomogeneous half-space, the proportion of concentrated load to total load on the footing, and the aspect ratio.

Displacement compatibility between the footing and foundation, as well as the requirement that the foundation be tensionless, reduces the unilateral contact problem under consideration to the solution of three coupled singular integral equations. The displacement and contact pressure inequalities make the problem nonlinear, and the iterative solution proceeds by first assuming the whole footing is in contact. The contact behavior expected in this class of problems was characterized and identified by Dundurs (1975); since the contact surface associated with the loaded configuration is contained within the initial contact surface, *receding* contact is observed. A general feature of smooth receding contact is for the extent of contact to be independent of the level of loading. Moreover, if uplift is to occur, the change from initial contact (the flat footing initially has all of its surface in contact) to the contact region in the loaded configuration takes place discontinuously.

Non-Hertzian or large-area contact problems generally have to be solved by means of numerical techniques. Hartnett (1980) developed an approach in which the area of contact is divided into a number of rectangular patches. The pressure in each patch is assumed to be uniform but unknown. The basic scheme developed by Hartnett has been extended and applied extensively (Ahmadi *et al.*, 1983). The numerical scheme formulated by Hartnett (1980) assumed the pressure in each rectangular patch to be constant but unknown. The advantage of this approach rested with an analytical integration of Boussinesq's fundamental solution over the patch being available in closed form in the case of a half-space (Love, 1929). However, in this paper the possible corner and edge singularities need special consideration. Rather than explicitly include these singularities, which is possible but computationally and analytically inconvenient, the authors chose to model the expected contact pressure singularities using adaptive discretization. The mesh spacing corresponds to the bi-directional singular behavior in such a way that integration of the contact pressure over each element gives the same constant if the pressure distribution is $C[(1-(2x/a)^2)(1-(2y/b)^2]^{-1/2}$.

BASIC EQUATIONS

A thin rectangular footing of side lengths a, b in unbonded frictionless contact with a nonhomogeneous half-space is subjected to a load $q(x, y)$ and an unknown support reaction $p(x, y)$ (Fig. 1). The governing equation for the footing deflection $w_f(x, y)$ is given by

$$D\nabla^4 w_f(x, y) = q(x, y) - p(x, y), \tag{1}$$

where the flexural rigidity of the footing, D, equals $E_f h^3/12(1-\nu_f^2)$; h is the thickness of the footing; E_f and ν_f are the Young's modulus and the Poisson's ratio of the footing, respectively.

The corresponding moments and the vertical forces can be written as

$$M_x = -D(w_{f,xx} + \nu_f w_{f,yy}), \tag{2a}$$

$$M_y = -D(w_{f,yy} + \nu_f w_{f,xx}), \tag{2b}$$

$$M_{xy} = D(1-\nu_f) w_{f,xy}, \tag{2c}$$

$$V_x = -D(w_{f,xx} + (2-\nu_f) w_{f,yy})_{,x}, \tag{2d}$$

$$V_y = -D(w_{f,yy} + (2-\nu_f) w_{f,xx})_{,y}. \tag{2e}$$

If the footing edges are free and the load is symmetric about both x- and y-axes, the following boundary conditions have to be satisfied:

$$M_x = V_x = 0, \quad \text{for } x = \pm a/2, \quad -b/2 \leqslant y \leqslant b/2; \tag{3a, b}$$

$$M_y = V_y = 0, \quad \text{for } y = \pm b/2, \quad -a/2 \leqslant x \leqslant a/2. \tag{3c, d}$$

Vertical force equilibration also requires that

$$\iint q(x, y)\,\mathrm{d}x\,\mathrm{d}y = \iint p(x, y)\,\mathrm{d}x\,\mathrm{d}y. \tag{4}$$

In general, the boundary condition that the corner forces must equal zero should also be enforced. However, for the symmetric loading conditions considered here, the corner forces must either all point upward or all point downward, and thus they must be zero if the equilibrium condition in eqn (4) and the condition [eqn (3b, d)] of zero edge forces are both satisfied. Therefore the condition of zero corner forces is not needed.

For a nonhomogeneous elastic half-space with a linearly varying shear modulus $G(z) = G_0 + mz$ and a constant Poisson's ratio $\nu_0 = 1/3$ (expressions for general values of ν_0 could also be determined), the surface displacement due to a uniform normal surface pressure, q, over a circular area, $r \leqslant b$, is given by Awojobi and Gibson (1973) as

$$w_0(r) = \frac{qb}{2G_0} \int_0^\infty \frac{J_0(r\xi) J_1(b\xi)}{\xi} f(\beta\xi)\,\mathrm{d}\xi, \tag{5}$$

where $\beta = G_0/m$,

$$f(\beta\xi) = f(t) = \frac{t[K_1^2(t)-K_0^2(t)]+K_0(t)K_1(t)}{t^2[K_1^2(t)-K_0^2(t)]+2K_1^2(t)-tK_0(t)K_1(t)}, \tag{6}$$

and K_0, K_1 are modified Bessel functions. It can be shown that

$$f(0) = 0. \tag{7}$$

By using asymptotic expansions of the Bessel functions for large arguments (Abramowitz and Stegun, 1972), it can also be shown that

$$f(t \to \infty) = \frac{4}{3} - \frac{5}{3t} + O\left(\frac{1}{t^2}\right). \tag{8}$$

For a point load P at the origin, let $b \to 0$ and $qb^2\pi \to P$,

$$w_0(r) = \frac{P}{4\pi G_0}\int_0^\infty J_0(r\xi)f(\beta\xi)\,\mathrm{d}\xi. \tag{9}$$

This integral diverges at the point $r = 0$ because of the first two terms in eqn (8), which means physically that the surface displacement under the concentrated load is infinitely large. These singularities can be extracted by defining a function

$$g(t) = f(t) - \frac{4}{3} + \frac{5}{3}\frac{1-e^{-t}}{t}. \tag{10}$$

In eqn (10) $g(t)$ is a well-behaved function that decays at a rate of t^{-2} as t approaches infinity.

Function $g(t)$ given in eqn (10) can be approximated by a function $\hat{g}(t)$ as

$$\hat{g}(t) = \sum_{m=1}^{M} \alpha_m \mathrm{e}^{-m\gamma t}, \tag{11}$$

where α_m and γ are unknown constants to be determined by using the least-squares error criterion such that the error Q is minimized. Exponential decay is used in eqn (11) instead of algebraic because the resulting integrals can then be performed analytically.

$$Q = \sum_{n=1}^{N} \{g(t_n) - \hat{g}(t_n)\}^2. \tag{12}$$

Since $\hat{g}(\alpha)$ decays at the rate of $1/t^2$, only a finite region needs to be considered, such that $0 = t_1 < t_2 < \ldots < t_n = L$. Then,

$$Q = \sum_{n=1}^{N}\left\{g(t_n) - \sum_{m=1}^{M}\alpha_m \mathrm{e}^{\;m\gamma t_n}\right\}^2. \tag{13}$$

To determine the coefficients α_m, use the conditions

$$\frac{\partial Q}{\partial \alpha_k} = 0, \quad k = 1, 2, \ldots, M, \tag{14}$$

to give

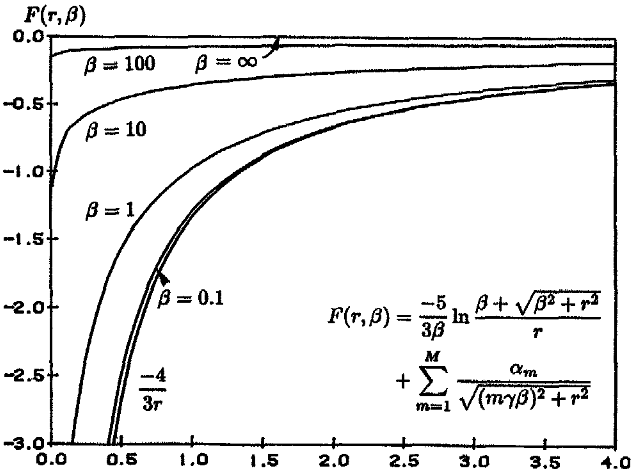

Fig. 2. Functions related to surface settlement due a point load.

$$\sum_{m=1}^{M}\alpha_m\left\{\sum_{n=1}^{N}e^{-(m+k)\gamma t_n}\right\}=\sum_{n=1}^{N}g(\alpha_n)e^{-k\gamma t_n},\quad k=1,2,\ldots,M. \tag{15}$$

The above equations are just ordinary linear equations which can be solved by a standard method once γ is given. The value of γ may be searched iteratively as in a one-variable optimization procedure. The accuracy of the approximation can be checked easily by comparing $g(t_n)$ and $\hat{g}(t_n)$ directly. The accuracy increases as the number of the terms increases.

For $N = 50000$, $t_n = (n-1)/10$ and $M = 10$, the coefficients α_m $(m = 1,2,..,10)$ obtained are

$$0.91333,\quad -17.84922,\quad 207.39267,\quad -1290.88357,\quad 4779.55271,$$
$$-10978.42693,\quad 15791.11701,\quad -13834.62563,\quad 6748.12628,\quad -1404.98258.$$

Also $\gamma = 0.26615$, $\max|g(t_n)-\hat{g}(t_n)| = 0.008$, $\sqrt{Q/N} = 0.0004$.

The integral in eqn (9) can be evaluated analytically after substituting $f(t)$ by the expressions in eqns (10) and (11) as

$$\begin{aligned}w_0(r)&=\frac{P}{4\pi G_0}\int_0^\infty J_0(r\xi)\left\{\frac{4}{3}-\frac{5}{3}\frac{1-e^{-\beta\xi}}{\beta\xi}+\hat{g}(\beta\xi)\right\}d\xi\\&=\frac{P}{4\pi G_0}\left\{\frac{4}{3r}-\frac{5}{3\beta}\ln\frac{\beta+\sqrt{\beta^2+r^2}}{r}+\sum_{m=1}^{M}\frac{\alpha_m}{\sqrt{(m\gamma\beta)^2+r^2}}\right\}.\end{aligned} \tag{16}$$

The first term in eqn (16) corresponds to the well known Boussinesq's solution of a point load on an elastic half-space, while the remaining terms related to β can be considered as correcting terms due to the nonhomogeneity. It can be seen that the correcting terms become zero for a homogeneous half-space ($\beta \to \infty$). These relations can be clearly seen from Fig. 2. The differences between the $-4/(3r)$ line and $F(r,\beta)$ line is the surface displacement of a nonhomogeneous half-space under a concentrated load.

The surface displacement of the foundation, $w_0\ (x,y)$, under a distributed contact pressure, $p(x,y)$, is now expressed by

$$w_0(x,y) = \frac{1}{3G_0}\int_{-b/2}^{b/2}\int_{-a/2}^{a/2} p(u,v)g(x,y;u,v)\,\mathrm{d}u\,\mathrm{d}v, \tag{17a}$$

where

$$g(x,y;u,v) = \frac{1}{\pi\sqrt{(x-u)^2+(y-v)^2}} + \frac{1}{\pi}H(\sqrt{(x-u)^2+(y-v)^2},\beta), \tag{17b}$$

in which

$$H(r,\beta) = \left\{-\frac{5}{4\beta}\ln\frac{\beta+\sqrt{\beta^2+r^2}}{r} + \frac{3}{4}\sum_{m=1}^{M}\frac{\alpha_m}{\sqrt{(m\gamma\beta)^2+r^2}}\right\}. \tag{17c}$$

Finally, in addition to the above equations, the compatibility conditions between the footing and the foundation must also be considered. Since the contact is unilateral, the support reaction is either compressive or zero. These conditions can be written as, with Ω denoting the contact region,

$$w_0(x,y) = w_f(x,y), \quad p(x,y) > 0, \quad \text{for } (x,y)\in\Omega; \tag{18a, b}$$

$$w_0(x,y) > w_f(x,y), \quad p(x,y) = 0, \quad \text{for } (x,y)\notin\Omega. \tag{18c, d}$$

RIGID RECTANGULAR FOOTING

For a symmetrically loaded rigid rectangular footing with side lengths of a and b, the surface displacement δ under the footing can be written as

$$\delta = \int_{-a/2}^{a/2}\int_{-b/2}^{b/2} w_0(\sqrt{(x-u)^2+(y-v)^2})p(u,v)\,\mathrm{d}u\,\mathrm{d}v, \quad |x|\leqslant a/2, \quad |y|\leqslant b/2, \tag{19}$$

where $p(u,v)$ is the contact pressure between the footing and the foundation. The title problem has been transformed into the solution of the integral equation for the unknown function $p(u,v)$.

The contact pressure is singular at the edges and corners of a rigid footing; for frictionless contact conditions, the singularities are asymptotical to $\rho^{-0.5}$ (Dundurs and Lee, 1972) and $\rho^{-0.7304}$ (Bažant, 1974) for the edges and corners, respectively (ρ is a local coordinate). The singularities decrease as β becomes smaller, and eventually disappear as $\beta \to 0$ (as for a Winkler foundation).

In order to treat these singularities, the method used in this paper is to discretize the contact region according to the Gauss–Chebyshev quadrature, which treats inverse-square-root edge singularities (the most singular case). As shown in Fig. 3, the footing is divided into N_E elements such that, for element j,

$$s_j \leqslant u \leqslant s_{j+1}, \quad t_j \leqslant v \leqslant t_{j+1}, \tag{20a, b}$$

where

$$s_j = \frac{a}{2}\cos\frac{(N_x-j_x+1)\pi}{N_x}, \quad t_j = \frac{b}{2}\cos\frac{(N_y-j_y+1)\pi}{N_y}. \tag{21a, b}$$

The compatibility condition is enforced at the element centers defined as

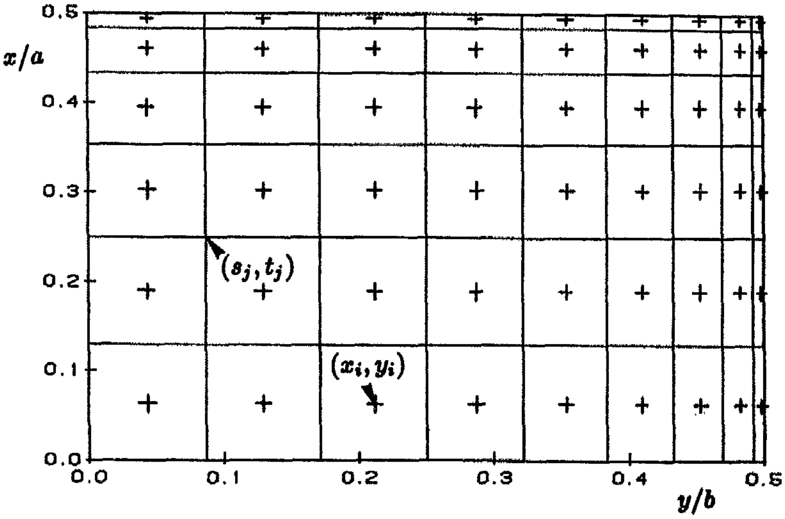

Fig. 3. Discretization scheme, $N_x = 12$, $N_y = 18$, $b/a = 3/2$.

$$x_i = \frac{a}{2}\cos\frac{(2N_x - 2i_x + 1)\pi}{2N_x}, \quad y_i = \frac{b}{2}\cos\frac{(2N_y - 2i_y + 1)\pi}{2N_y}. \tag{21c, d}$$

N_x, N_y are the numbers of the elements in the x, y directions; and i_x, i_y, j_x, j_y are the sequential numbers in the two directions, respectively. Next, the contact pressure $p(x, y)$ is assumed constant in each element. In this way, eqn (19) gives rise to the following system of linear equations:

$$\sum_{j=1}^{N_E} B_{ij} p_j = \delta, \quad i = 1, 2, \ldots, N_E, \tag{22}$$

where

$$B_{ij} = \int_{t_j}^{t_{j+1}} \int_{s_j}^{s_{j+1}} w_0(x_i, y_i; u, v)\, du\, dv, \tag{23}$$

and p_j is the center pressure in element j. Upon substituting eqn (16) into eqn (23), all integrals can be evaluated analytically (see Appendix), except the integrals involving $\ln(\beta + \sqrt{\beta^2 + r^2})$, which are evaluated numerically by using Gauss quadrature since the logarithmic function of r is a regular function for $\beta \neq 0$.

From the equilibrium condition,

$$\sum_{j=1}^{N_E} A_j p_j = P_0, \tag{24}$$

where P_0 is the total load and A_j is the area of element j. Once δ or P is given, the $N_E + 1$ unknowns can be solved from eqns (22) and (24).

The above method of adaptive discretization has the feature that, if the function $p(x, y)$ is proportional to $\{[1 - (2x/a)^2][1 - (2y/b)^2]\}^{-1/2}$, the integration of $p(x, y)$ over each element contributes the same amount. Thus the increasing rate of change of the function near the edges has been taken into account. The pressure singularities at the corners are overestimated, since they are less singular than ρ^{-1}. The edge singularity is also overestimated for a foundation with a finite β. For full contact, the singular pressure distribution is approximated here by a piecewise constant function. The piecewise constant pressures tend to infinity as the edge of the footing is approached; the edge of the associated element tends

Table 1. Convergence study for a rigid square footing, $(\delta/a)(E_0/p_{av})$

$\beta/a =$	∞	100	10	1	0.1
$N_x = N_y = 8$	0.771328	0.753549	0.673807	0.429644	0.145046
$N_x = N_y = 16$	0.771378	0.753603	0.673883	0.429841	0.145278
$N_x = N_y = 32$	0.771399	0.753624	0.673907	0.429879	0.145340

to zero. The net force and displacements (Table 1) are accurately predicted, while the contact pressure is truncated right at the edge. Nevertheless, this adaptive discretization scheme works very well; by this scheme, most of the required integrations are completed in this paper in closed form. This is very important in a study that necessitates iteration to find the correct contact area.

RIGID STRIP FOOTING

The problem of a rigid strip footing ($b/a = \infty$) can be treated in a similar way as the rectangular footing. The contact pressure is singular again at the edges. Therefore, by dividing the footing into a number of elements along the length according to eqns (20), (21a, c), and assuming the contact pressure is constant in each element, equations similar to eqns (22), (23) and (24) can be derived.

For a nonhomogeneous half-space loaded uniformly along an infinite strip $|x| < b$, the surface displacement can be expressed as (Awojobi and Gibson, 1973)

$$w_0(x) = \frac{q}{\pi G_0} \int_0^{\infty} \frac{\sin(b\xi)\cos(x\xi)}{\xi^2} f(\beta\xi)\,\mathrm{d}\xi. \tag{25}$$

To obtain the shape of surface settlement, the difference of settlement can be expressed as

$$\begin{aligned} w_0(x) - w_0(0) &= \frac{-q}{\pi G_0} \int_0^{\infty} \frac{1-\cos(x\xi)}{\xi^2} \sin(b\xi) f(\beta\xi)\,\mathrm{d}\xi \\ &= \frac{-q}{\pi G_0} \int_0^{\infty} \frac{1-\cos(x\xi)}{\xi^2} \sin(b\xi) \left\{ \frac{4}{3} - \frac{5}{3}\,\frac{1-\mathrm{e}^{-\beta\xi}}{\beta\xi} + \sum_{m=1}^{M} \alpha_m \mathrm{e}^{-m\gamma\beta\xi} \right\} \mathrm{d}\xi. \end{aligned} \tag{26}$$

The different integrals in eqn (26) can all be evaluated analytically (see Appendix).

With eqn (26), the surface settlement at a point due to the uniform load at an element can be calculated through appropriate coordinate transformations.

Shown in Tables 2 and 3 are the displacement and center contact pressure of a rigid rectangular footing on a nonhomogeneous elastic half-space, respectively. For $\beta/a = \infty$, the values in the tables are the same as those of the homogeneous half-space (Dempsey and Li, 1989a). Also, for $\beta/a = \infty$ and $b/a = \infty$, it can be checked that $p(0, 0)/p_{av} = 2/\pi$ (Sadowsky, 1928). The limiting case of $b/a = \infty$ is calculated for a rigid strip footing as described above. All terms are nondimensional. It is especially interesting to note the term β/a: the nonhomogeneity can be scaled with respect to the side length of the footing. This

Table 2. Displacement of a rigid rectangular footing $(\delta/a)(E_0/p_{av})$

$\beta/a =$	∞	100	10	1	0.1
$b/a = 1.0$	0.7714	0.7536	0.6739	0.4299	0.1453
$b/a = 1.5$	0.9366	0.9111	0.8012	0.4877	0.1556
$b/a = 2.0$	1.0638	1.0311	0.8944	0.5263	0.1617
$b/a = 3.0$	1.2553	1.2091	1.0263	0.5760	0.1686
$b/a = 5.0$	1.5129	1.4427	1.1867	0.6289	0.1749

$\delta \to \infty$ when $\beta = 0$ or $r = \infty$; $E_0 = 8G_0/3$; $\nu_0 = 1/3$.

Table 3. Center pressure of a rigid rectangular footing $p(0, 0)/p_{av}$

$\beta/a =$	∞	100	10	1	0.1
$b/a = 1.0$	0.4851	0.4868	0.5006	0.5776	0.7403
$b/a = 1.5$	0.4879	0.4899	0.5061	0.5929	0.7519
$b/a = 2.0$	0.4940	0.4963	0.5140	0.6049	0.7633
$b/a = 3.0$	0.5057	0.5084	0.5281	0.6238	0.7806
$b/a = 5.0$	0.5223	0.5255	0.5484	0.6466	0.8000
$b/a = \infty$	0.6366	0.6386	0.6540	0.7254	0.8434

$p(0,0)/p_{av} = 1$ when $\beta = 0$; $v_0 = 1/3$.

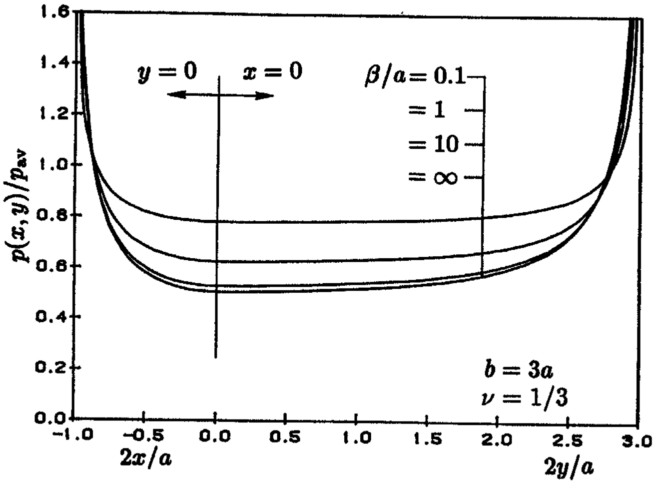

Fig. 4. Contact pressure of a rigid footing with different β/a values.

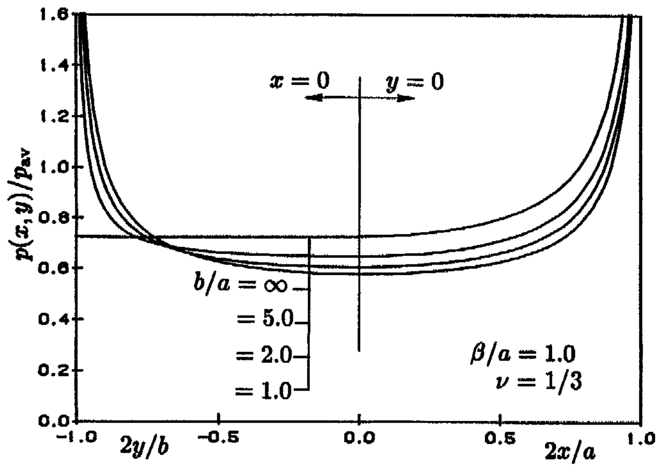

Fig. 5. Contact pressure of a rigid footing with different aspect ratio, b/a.

means that, for a given β, the foundation appears stiffer as the footing becomes larger. Theoretically, for $\beta \to 0$, the surface displacement becomes infinite and contact pressure becomes uniform. However, from Table 3 it can be seen that the contact pressure is still far from that for a Winkler foundation ($p(x, y)/p_{av} \equiv 1$). Since $\beta/a = 0.1$ means that the shear modulus of the foundation at a depth equal to the side length of the footing is 11 times greater than at the surface, smaller values of β/a are not likely to be physically meaningful. As mentioned previously, $\beta = \infty$ corresponds to the case of a homogeneous half-space.

The contact pressure distributions for different aspect ratios and β/a values are shown in Figs 4 and 5, respectively. The contact pressure tends to be more uniform as β/a decreases.

It is important to note that the aspect ratio has only a minor influence on the contact pressure distribution.

FLEXIBLE RECTANGULAR FOOTINGS

A completely rigid footing does not exist in reality, since every footing has a certain finite flexibility. The question then arises naturally: how rigid must a footing be in order to be treated as rigid? One possible standard to make such a judgement is to compare the center pressure and displacement of a flexible footing with those values for a rigid footing.

In the case of finite flexibility, the solution of the footing deflection (w_f) can be expressed as follows: a particular solution (w_1) due to the support reaction $p(x, y)$, a particular solution (w_2) due to the applied load $q(x, y)$, a complementary solution (w_3) and the corner deflection (δ). Hence

$$\begin{aligned} w_f(x,y) &= w_1(x,y)+w_2(x,y)+w_3(x,y)+\delta \\ &= \frac{-a^3}{bD}\int_{-b/2}^{b/2}\int_{-a/2}^{a/2} p(u,v)f(x,y;u,v)\,\mathrm{d}u\,\mathrm{d}v \\ &\quad +\frac{a^3}{bD}\int_{-b/2}^{b/2}\int_{-a/2}^{a/2} q(u,v)f(x,y;u,v)\,\mathrm{d}u\,\mathrm{d}v \\ &\quad +a\sum_{i=1,3,}^{\infty}\{A_i\cosh\alpha_i y+B_i\alpha_i y\sinh\alpha_i y\}\,\mathrm{sech}\,\eta_i\cos\alpha_i x \\ &\quad +a\sum_{j=1,3,}^{\infty}\{C_j\cosh\beta_j x+D_j\beta_j x\sinh\beta_j x\}\,\mathrm{sech}\,\xi_j\cos\beta_j y+\delta, \end{aligned} \tag{27}$$

where

$$f(x,y;u,v)=\frac{4}{\pi^4}\sum_{m=1,3}^{\infty}\sum_{n=1,3,}^{\infty}\frac{\cos\alpha_m x\cos\beta_n y\cos\alpha_m u\cos\beta_n v}{(m^2+(n/r)^2)^2}, \tag{28}$$

$$\alpha_k=\frac{k\pi}{a},\quad \beta_k=\frac{k\pi}{b},\quad \xi_k=\frac{k\pi a}{2b},\quad \eta_k=\frac{k\pi b}{2a}. \tag{29}$$

The terms sech η_i and sech ξ_j are added for mathematical convenience; $w_2(x, y)$ can be calculated for any given load.

The coefficients A_i, B_i, C_j, D_j can be determined from the boundary conditions in eqn (3). The zero moment conditions (3a,c) give A_i and C_j in terms of B_i and D_j, respectively. The zero vertical force conditions (3b,d) give two more equations to evaluate B_i and D_j. The variables x and y within these equations can be removed as follows: multiply both sides of the first equation by $(2b^2/a\pi^3 D)\cos\beta_k y$, ($k = 1, 3, \dots$), and integrate from $-b/2$ to $b/2$ with respect to y; multiply both sides of the second equation by $(2a/\pi^3 D)\cos\alpha_l x$, ($l = 1, 3, \dots$), and integrate from $-a/2$ to $a/2$ with respect to x. Thus eqns (30) and (31) in the following are derived.

Another equation can be derived from the compatibility conditions by substituting eqns (27) and (5a,e) into eqn (18a,d) to give eqn (32) in the following. The title contact problem has thus been reduced to the solution of the following three coupled two-dimensional singular integral equations, in which the remaining unknowns are $p(x, y)$, B_i ($i = 1, 3, \dots$), D_j ($j = 1, 3, \dots$) and the extent of contact, Ω:

$$\frac{a^2}{bD}\iint_{\Omega} p(u,v)\phi_k(u,v)\,\mathrm{d}u\,\mathrm{d}v + \sum_{i=1,3,}^{\infty} E_{ki}B_i + G_k D_k = I_k, \quad k = 1,3,\ldots \tag{30}$$

$$\frac{a^2}{bD}\iint_{\Omega} p(u,v)\theta_l(u,v)\,\mathrm{d}u\,\mathrm{d}v + \sum_{j=1,3,}^{\infty} F_{lj}D_j + H_l B_l = J_l, \quad l = 1,3,\ldots \tag{31}$$

$$\frac{a^3}{bD}\iint_{\Omega} p(u,v)f(x,y;u,v)\,\mathrm{d}u\,\mathrm{d}v + \frac{1}{3\pi G_0}\iint_{\Omega}\frac{p(u,v)\,\mathrm{d}u\,\mathrm{d}v}{\sqrt{(x-u)^2+(y-v)^2}}$$

$$+\frac{1}{3\pi G_0}\iint_{\Omega} p(u,v)F(\sqrt{(x-u)^2+(y-v)^2},\beta)\,\mathrm{d}u\,\mathrm{d}v$$

$$-a\sum_{i=1,3,}^{\infty} B_i\lambda_i(x,y) - a\sum_{j=1,3,}^{\infty} D_j\psi_j(x,y) = w_2(x,y)+\delta, \quad x,y\in\Omega. \tag{32}$$

The constants and functions in eqns (32–34) are defined as follows:

$$E_{ki} = k^3 i^3(1-v_f)(8/r\pi)\sin\gamma_i\sin\gamma_i/(i^2+(k/r)^2)^2, \tag{33a}$$

$$F_{lj} = l^3 j^3(1-v_f)(8r/\pi)\sin\gamma_l\sin\gamma_j/(j^2+(lr)^2)^2, \tag{33b}$$

$$G_k = k^3(1-v_f)(\xi_k\,\mathrm{sech}^2\,\xi_k - \zeta_p\tanh\xi_k), \tag{33c}$$

$$H_l = l^3(1-v_f)(\eta_l\,\mathrm{sech}^2\,\eta_l - \zeta_p\tanh\eta_l), \tag{33d}$$

$$I_k = \frac{a^3r^3}{\pi^4 D}\sum_{m=1,3,}^{\infty} b_{mk}\frac{m(m^2+(2-v_f)(k/r)^2)\sin\gamma_m}{(m^2+(k/r)^2)^2}, \tag{33e}$$

$$J_l = \frac{a^3 r}{\pi^4 D}\sum_{n=1,3,}^{\infty} b_{ln}\frac{n(n^2+(2-v_f)(lr)^2)\sin\gamma_n}{(n^2+(lr)^2)^2}, \tag{33f}$$

$$\phi_k(u,v) = \frac{4r^3}{\pi^4}\sum_{m=1,3,}^{\infty}\frac{m(m^2+(2-v_f)(k/r)^2)}{(m^2+(k/r)^2)^2}\cos\alpha_m u\cos\beta_k v\sin\gamma_m, \tag{33g}$$

$$\theta_l(u,v) = \frac{4r}{\pi^4}\sum_{n=1,3,}^{\infty}\frac{n(n^2+(2-v_f)(lr)^2)}{(n^2+(lr)^2)^2}\cos\alpha_l u\cos\beta_n v\sin\gamma_n, \tag{33h}$$

$$\lambda_i(x,y) = \{\alpha_i y\sinh\alpha_i y - (\mu_p+\eta_i\tanh\eta_i)\cosh\alpha_i y\}\,\mathrm{sech}\,\eta_i\cos\alpha_i x, \tag{33i}$$

$$\psi_j(x,y) = \{\beta_j x\sinh\beta_j x - (\mu_p+\xi_j\tanh\xi_j)\cosh\beta_j x\}\,\mathrm{sech}\,\xi_j\cos\beta_j y, \tag{33j}$$

$$b_{ij} = \frac{4}{ab}\int_{-b/2}^{b/2}\int_{-a/2}^{a/2} q(x,y)\cos\alpha_i x\cos\beta_j y\,\mathrm{d}x\,\mathrm{d}y, \tag{33k}$$

$$r = \frac{b}{a},\quad \gamma_k = \frac{k\pi}{2},\quad \zeta_p = \frac{3+v_f}{1-v_f},\quad \mu_p = \frac{2}{1-v_f}. \tag{33l}$$

Since the problem is nonlinear, iteration has to be used. The following procedure is used in this paper:

(1) assume a contact region Ω;
(2) for the given region solve for $p_i = p(x_i, y_i)$ and δ;
(3) check eqn (18b) and, if necessary, find a new Ω which excludes the areas where the support reaction is in tension;

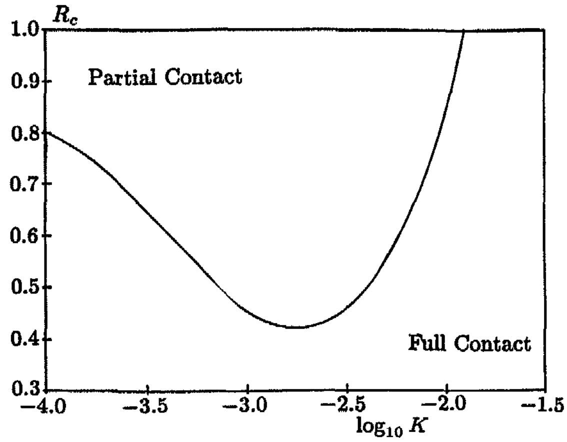

Fig. 6. Critical load ratio for uplift to occur ($\beta = \infty$, $b = a$, $\nu_f = \nu_0 = 1/3$).

(4) finally, check eqn (18c) and, if necessary, find a new Ω which includes the areas where the footing is in contact with the foundation, i.e. $w_f(x, y) \geqslant w_0(x, y)$.

Because the load and deflection are symmetric, they need to be calculated only over a quarter of the footing, e.g. over an area of $0 \leqslant x \leqslant a/2$, $0 \leqslant y \leqslant b/2$. The matrices are rearranged each time to eliminate the extra unknown variables and equations in order to conform with eqn (18a,d). The matrix elements, however, need to be calculated only once.

A nondimensional stiffness ratio K is introduced as

$$K = \frac{1}{12} \frac{E_f(1-\nu_0^2)}{E_0(1-\nu_f^2)} \left(\frac{h}{a}\right)^3, \tag{34}$$

where h is thickness of the footing, E_f is the elastic modulus of the footing, and E_0 is the surface elastic modulus of the half-space. For a concrete footing on soil, sand or gravel with $a/h = 5$–10, $E_0 = 10$–20 ksi, $E_f = 3000$–4500 ksi, $K = 0.006$–0.333 and $\log_{10} K = -2.2$ to -0.5. It can be seen that the K-values depend strongly on the thickness to width ratio, h/a.

The contact behavior of a flexible footing on an elastic foundation is strongly influenced by the loading configuration. The particular cases of combined loads of a uniform load (self-weight) q_0 and a centrally concentrated load P_0 are studied in the following; the proportion of the concentrated load is identified by the load ratio R, where

$$R = P_0/(P_0 + q_0 ab). \tag{35}$$

The influences of flexibility of the footing K and the load ratio R have been thoroughly ascertained for rectangular footings on a *homogeneous* half-space ($\beta = \infty$) or a Winkler foundation ($\beta = 0$) (Li and Dempsey, 1988; Dempsey and Li, 1989a,b). The understanding thereby gained is now briefly summarized. Full contact and the associated linear response are always maintained until the proportion of the concentrated load is greater than a critical value R_c (Fig. 6). Reducing the R-value always tends to bring the footing into full contact with the foundation. However, increasing the stiffness ratio K does not always imply a more rigid condition. A very stiff—or rigid—footing is obtained if $\log_{10} K > -1.5$. As the footing becomes more flexible, with $-2.5 < \log_{10} K < -1.5$, the reduction in K does physically lead to more uplift, as is intuitively expected. The trend reverses, however, if the footing becomes even more flexible, with $\log_{10} K < -2.5$. This reversal happens because the self-weight or distributed load exerts an increasingly dominant influence in this case. If the footing were infinitely flexible, for instance, no uplift would occur at all. The complicated interaction between K and R is illustrated for the case of a square footing on a homogeneous

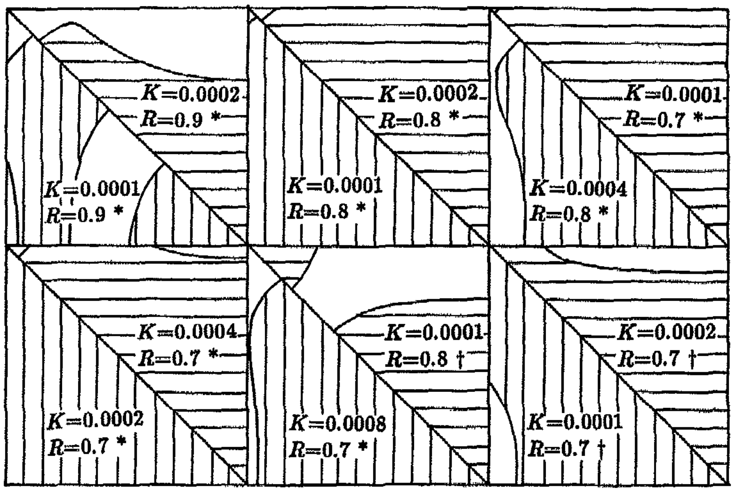

Fig. 7. Contact regions for very flexible square footings (* homogeneous half-space, † Winkler foundation).

half-space and a Winkler foundation in Fig. 7 (the * and † indicate an elastic half-space and a Winkler foundation, respectively).

For the case of a square footing resting on a homogeneous half space (Li and Dempsey, 1988) and subjected solely to a concentrated load, the contact regions are circles or parts of circles if the edges are in contact (Fig. 8). The contact regions for rectangular footings on an elastic half-space are shown in Fig. 6 of Dempsey and Li (1989b). The contact regions without any distributed load are elliptical. It is interesting to note that the major axis of the ellipse is in the short direction of the footing because it is easier to bend about the short direction. For flexible footings on a homogeneous half-space with distributed loads, the contact regions are very irregular; the footing can have a central contact region, lose contact, then regain contact.

Returning to the title problem and the nonhomogeneous half-space, the magnification of the center pressure and displacement are given in Figs 9 and 10, respectively, for the cases of a centrally concentrated load only and a uniform load only. As may be expected, the influence of footing rigidity is small for a uniform load, even for infinitely flexible footings (see inserted tables). This means that a rather flexible footing can be considered rigid if subjected to a uniform load only. For a concentrated load, the differences between the rigid footing solution and the flexible footing solution may be very large, e.g. over 60%

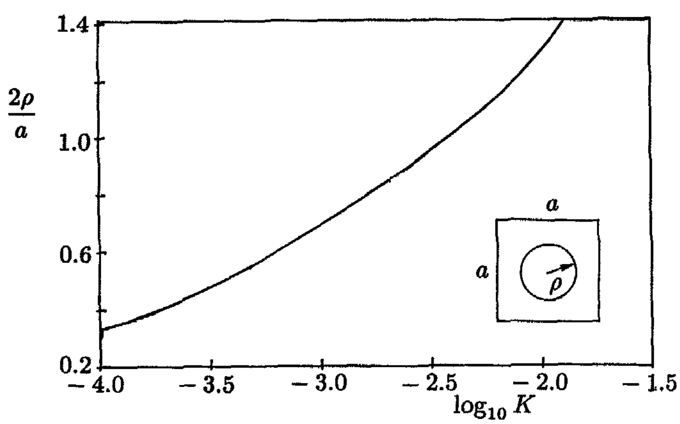

Fig. 8. Contact radii for a square footing on a homogeneous half-space ($R = 1$, $b = a$, $\nu_f = 0.3$).

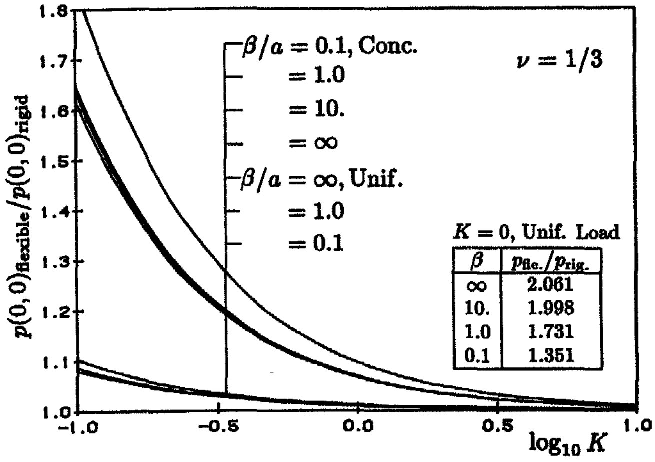

Fig. 9. Magnification of center pressure due to the footing flexibility.

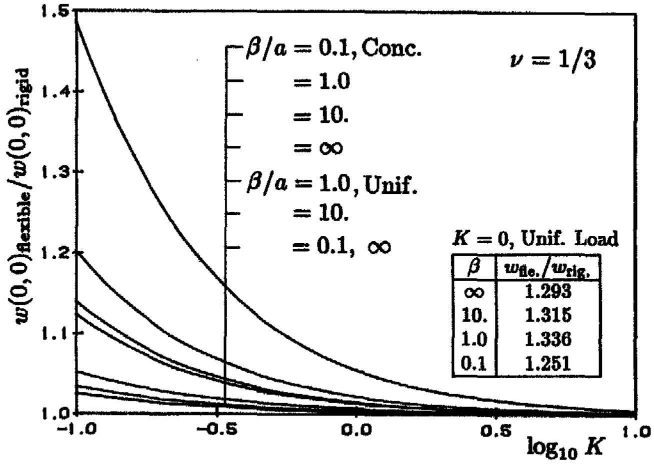

Fig. 10. Magnification of center displacement due to the footing flexibility.

for $K = 0.1$. Note that superposition can be used for cases of combined loads. Therefore, the load type should be taken into account when considering the rigidity of a footing. As a general rule, from the viewpoint of center displacement and center contact pressure, a footing may considered rigid if $K > 1$.

Another way to consider a footing as rigid is to check if uplift occurs or is impending. However, from previous results (Li and Dempsey, 1988), it can be found that uplift occurs only if the footing is very flexible. For instance, for a square footing on a homogeneous elastic half-space, uplift occurs if $K \leqslant 0.01$. For $K = 0.01$, the center settlement of the flexible footing is twice that of a rigid footing and the center contact pressure is five times greater.

The changes in contact pressure distributions are shown in Fig. 11. Clearly, a smaller β/a ratio has about the same effect as a smaller K value, viz., a faster increase in the elastic modulus makes the footing relatively more flexible.

APPROXIMATE CONTACT PRESSURE DISTRIBUTIONS

It can be seen from the figures that the contact pressure distributions are all similar. Therefore, an approximate expression may be suggested for practical uses. For example, for a rectangular footing

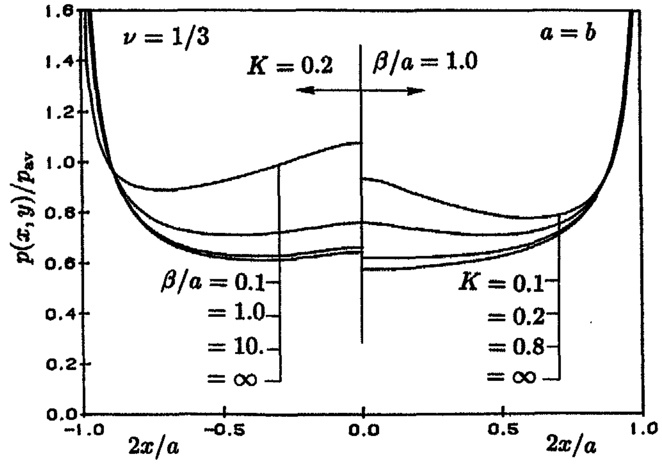

Fig. 11. Contact pressure of a flexible square footing with different β/a and K values.

$$\frac{p(x,y)}{p_{av}} = \frac{A + B[(2x/a)^2 + (2y/b)^2]}{\sqrt{1-(2x/a)^2}\sqrt{1-(2y/b)^2}}, \tag{36}$$

the constants A and B can be determined by requiring that the approximate expression has the same resultant force and the center value as the exact solution. Thus

$$A = P_c, \quad B = \frac{4}{\pi^2} - P_c, \quad P_c = \frac{p(0,0)}{p_{av}}. \tag{37}$$

Then, by finding or interpolating the P_c values from Table 2, and modifying them using Fig. 10, if the footing is flexible, an approximate pressure distribution can be obtained.

For a strip footing, the following expression can be used

$$\frac{p(x)}{p_{av}} = \frac{A + B(2x/a)^2}{\sqrt{1-(2x/a)^2}}, \quad A = P_c, \quad B = \frac{4}{\pi} - 2A. \tag{38}$$

These expressions can be used to estimate the bending moments and shear forces.

CONCLUSIONS

The problem of a rigid rectangular footing on a nonhomogeneous foundation can be formulated into an integral equation and solved numerically.

The following conclusions can be drawn from the numerical results:

(1) Increasing the value of m in $G(z) = G_0 + mz$ reduces the foundation settlement considerably and makes the contact pressure more uniform.

(2) A parameter, $\beta/a = G_0/(am)$, can be introduced to indicate the degree of nonhomogeneity. It is important to notice that increasing the side length a has a similar effect as increasing the nonhomogeneity parameter m. In other words, the nonhomogeneity considered is more important for larger footings.

(3) Theoretically, a Winkler foundation is the limiting case for the nonhomogeneous foundation with an infinite m/G_0 value. However, it has been found that the two foundations behave quite differently for any practical m/G_0 values.

(4) Since the contact pressure is theoretically singular at the edges, the traditional assumption of uniform pressure distribution may significantly underestimate the central bending moment.

(5) If the proportion of the centrally concentrated load to the total load is large, the flexibility of the footing should be considered even for a concrete footing on soil. The stiffness ratio K is a key indicator, in which the ratio h/a is an important number.

REFERENCES

Abramowitz, M. and Stegun, I. A. (1972). *Handbook of Mathematical Functions*. Dover New York.

Ahmadi, N., Keer, L. M. and Mura, T. (1983). Non-Hertzian contact stress analysis for an elastic half space—normal and sliding contact. *Int. J. Solids Structures*. **19**, 357–373.

Awojobi, A. O. and Gibson, R. E. (1973). Plane strain and axially symmetric problems of a linearly non-homogeneous elastic half space. *Q. J. Mech. Appl. Math.* **26**, 285–302.

Bažant, Z. P. (1974). Three-dimensional harmonic functions near termination or intersection of gradient singularity lines: a general numerical method. *Int. J. Eng. Sci.* **12**, 221–243.

Boswell, L. F. and Scott, C. R. (1976). A flexible circular footing on a hetrogeneous elastic half-space: influence coefficient for contact stress and settlement. *Géotechnique* **30**, 604–610.

Brown, P. T. (1969). Numerical analysis of uniformly loaded circular raft on deep elastic foundation. *Géotechnique* **23**, 67–84.

Brown, P. T. and Gibson, R. E. (1972). Surface settlement of a deep elastic stratum whose modulus increases linearly with depth. *Can. Geot. J.* **9**, 467–476.

Brown, P. T. (1974). Influence of soil inhomogeneity on raft behaviour. *Soil Found.* **14**, 61–70.

Brown, P. T. and Gibson, R. E. (1973). Rectangular loads on inhomogeneous elastic soil. *ASCE J. Soil Mech. Found. Div.* **99**, 917–970.

Brown, P. T. and Gibson, R. E. (1979). Surface settlement of a finite elastic layer whose modulus increases linearly with depth. *Int. J. Numer. Anal. Meth. Geom.* **3**, 37–47.

Burland, J. B., Gilliane, C. S. and Gibson, R. E. (1973). A field and theoretical study of the influence of non-homogeneity on settlement. *Proc. 8th Int. Conf. Soil Mechanics*, Moscow, vol. 1.3, pp. 39–84.

Carrier, W. D. and Christian, J. T. (1973). Rigid circular footing resting on a non-homogeneous elastic half-space. *Géotechnique* **23**, 67–84.

Dempsey, J. P. and Li, H. (1989a). A rigid rectangular footing on an elastic layer. *Géotechnique* **39**, 147–152.

Dempsey, J. P. and Li, H. (1989b). A flexible rectangular footing on an elastic layer: large area contact. *ASME J. Trib.* **111**, 518–524.

Dundurs, J. (1975). Properties of elastic bodies in contact. In *The Mechanics of the Contact between Deformable Bodies* (Edited by A. D. De Pater and J. J. Kalker). Delft University Press.

Dundurs, J. and Lee, M.-S. (1972). Stress concentration at a sharp edge in contact problems. *J. Elast.* **2**, 109–112.

Gibson, R. E. (1969). Some results concerning displacement and stresses in a nonhomogeneous half-space. *Géotechnique* **17**, 58–67.

Gibson, R. E. (1974). The analytical method in soil mechanics. *Géotechnique* **24**, 115–144.

Gibson, R. E., Brown, P. T. and Andrews, K. R. F. (1971). Some results concerning displacement in a non-homogeneous elastic layer. *J. Appl. Math. Phys. (ZAMP)* **22**, 885–964.

Hartnett, M. (1980). A general numerical solution for elastic body contact problems. In *Solid Contact and Lubrication* (Edited by H. S. Cheng and L. M. Keer). ASME AMD—**39**, 51–66.

Li, H. and Dempsey, J. P. (1988). Unbonded contact of a square footing on an elastic half-space or a Winkler foundation. *ASME J. Appl. Mech.* **55**, 430–436.

Love, A. E. H. (1929). The stress potential in a semi-infinite solid by pressure on part of the boundary. *Phil. Trans. R. Soc. Lond. Ser. A* **228**, 377–420.

Lur'e, A. I. (1964). *Three-Dimensional Problems of the Theory of Elasticity*. Interscience, New York.

Sadowsky, M. (1928). Zweidimensionale Probleme der Elastizitätstheorie. *J. Appl. Math. Mech. (ZAMM)* (in German) **8**, 107–121.

APPENDIX: ANALYTACAL INTEGRATIONS

$$\int_{s_1}^{s_2}\int_{t_1}^{t_2}\frac{\mathrm{d}u\,\mathrm{d}v}{\sqrt{(x-u)^2+(y-v)^2}} = I_1(s_1-x, s_2-x, t_1-y, t_2-y), \tag{A1}$$

$$\int_{s_1}^{s_2}\int_{t_1}^{t_2}\ln\sqrt{(x-u)^2+(y-v)^2}\,\mathrm{d}u\,\mathrm{d}v = I_2(s_1-x, s_2-x, t_1-y, t_2-y), \tag{A2}$$

$$\int_{s_1}^{s_2}\int_{t_1}^{t_2}\frac{\mathrm{d}u\,\mathrm{d}v}{\sqrt{(x-u)^2+(y-v)^2+z^2}} = I_3(s_1-x, s_2-x, t_1-y, t_2-y), \tag{A3}$$

$$I_k(a,b,c,d) = f_k(a,c)+f_k(b,d)-f_k(a,d)-f_k(b,c), \tag{A4}$$

$$f_1(\alpha,\beta) = \alpha\ln(\sqrt{\alpha^2+\beta^2}+\beta)+\beta\ln(\sqrt{\alpha^2+\beta^2}+\alpha), \tag{A5}$$

$$f_2(\alpha,\beta) = \{\alpha\beta\ln(\alpha^2+\beta^2)-3\alpha\beta+\alpha^2\arctan(\beta/\alpha)+\beta^2\arctan(\alpha/\beta)\}/2, \tag{A6}$$

$$f_3(\alpha,\beta) = \frac{\alpha}{2}\ln\frac{\sqrt{\alpha^2+\beta^2+z^2}+\beta}{\sqrt{\alpha^2+\beta^2+z^2}-\beta} + \frac{\beta}{2}\ln\frac{\sqrt{\alpha^2+\beta^2+z^2}+\alpha}{\sqrt{\alpha^2+\beta^2+z^2}-\alpha}$$

$$-z\left\{\arcsin\frac{\alpha\beta}{\sqrt{\alpha^2+z^2}\,(\sqrt{\alpha^2+\beta^2+z^2}+z)} + \arcsin\frac{\alpha\beta}{\sqrt{\beta^2+z^2}\,(\sqrt{\alpha^2+\beta^2+z^2}+z)}\right\}, \quad \text{(A7)}$$

$$\int_0^\infty \frac{1-\cos(a\xi)}{\xi^2}\sin(b\xi)\,\mathrm{d}\xi = \frac{b}{2}\log\frac{|b^2-a^2|}{b^2} + \frac{a}{2}\log\left|\frac{b+a}{b-a}\right|, \quad \text{(A8)}$$

$$4\int_0^\infty \frac{1-\cos(a\xi)}{\xi^2}\sin(b\xi)\,\mathrm{e}^{-c\xi}\,\mathrm{d}\xi = (b+a)\log[(b+a)^2+c^2]+(b-a)\log[(b-a)^2+c^2]$$

$$+2c\arctan[(b+a)/c]+2c\arctan[(b-a)/c]-2b\log(b^2+c^2)-4c\arctan(b/c), \quad \text{(A9)}$$

$$4\int_0^\infty \frac{1-\cos(a\xi)}{\xi^2}\,\frac{1-\mathrm{e}^{-\beta\xi}}{\xi}\sin(b\xi)\,\mathrm{d}\xi = \beta(b+a)\log[(b+a)^2+\beta^2]+\beta(b-a)\log[(b-a)^2+\beta^2]$$

$$+(b+a)^2\arctan[\beta/(b+a)]+(b-a)^2\arctan[\beta/(b-a)]$$

$$+\beta^2\arctan[(b+a)/\beta]+\beta^2\arctan[(b-a)/\beta]$$

$$-2b^2\arctan(\beta/b)-2\beta^2\arctan(b/\beta)-2b\beta\log(b^2+\beta^2). \quad \text{(A10)}$$

Equation (A7) has been derived from Lur'e (1964).